

# Acoustic modeling of a Diesel Particulate Filter using a double equivalent fluid homogenization approach

Gregory Lielens<sup>1</sup>, Markus Brandstetter<sup>2</sup>, Alexis Talbot<sup>3</sup>

<sup>1</sup> Free Field Technologies, MSC Software Belgium, 1435 Mont-Saint-Guibert, E-Mail:Gregory.Lielens@fft.be

<sup>2</sup> Free Field Technologies, MSC Software Belgium, 1435 Mont-Saint-Guibert, E-Mail:Markus.Brandstetter@fft.be

<sup>3</sup> Free Field Technologies, MSC Software Belgium, 1435 Mont-Saint-Guibert, E-Mail:Alexis.Talbot@fft.be

## Introduction

In order to comply with more and more stringent engine particulate emission regulations, Diesel Particulate Filters (DPF) are used to filter polluting particulate and reduce pollutants in the exhaust gas of a car. These devices have a noticeable impact on the acoustic behavior of the exhaust line. It is therefore of interest to study their effect through numerical simulations.

In order to account for the effect of the DPF in a finite element acoustic simulation model, a double equivalent fluid homogenization is presented in this paper. It consists of two sets of duct arrays modeled with an anisotropic equivalent fluid model and coupled with local exchange admittance. This model accounts for visco-thermal dissipation in the ducts and the acoustic transmission between the two sets of duct arrays in presence of a mean flow.

In the present paper, the Double Visco-Thermal Array (DVTA) model is presented and then applied to a realistic case for which measurement results are available [1]. The acoustic transmission loss of the DPF is computed and compared to other modeling techniques and experimental results.

Compared to [2], the transfer matrix coupling two ducts contains the Bulk modulus, and investigations concerning the mean flow are shown.

## Diesel Particulate Filter

Emission control systems are located at the beginning of the exhaust line and consist of duct arrays. Those ducts allow the exhaust gas to pass through, being filtered on the passage. There are two different types of duct arrays, see Figure 1.

In the single duct array the air passes through one duct array only. Each duct array has an inlet and an outlet. Typical single duct array systems are catalytic converters and radiators.

In the double duct array such as the DPF the air passes through two ducts being connected through a porous material. The air is entering at the inlet of the first duct, passing through the porous material (e.g.: cordierite for DPF) and exits at a second duct array, see Figure 1. Heat exchangers are other systems based on a double duct array.

Single and double duct arrays have an important impact on the acoustic transmission of the exhaust line.

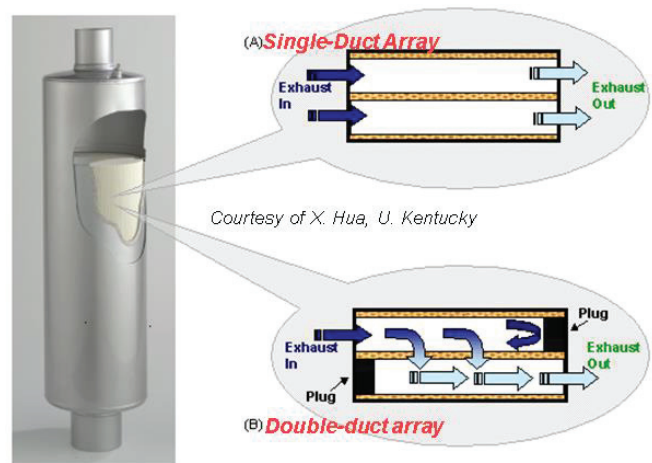


**Figure 1:** Types of duct arrays and the acoustic waves propagation direction [1]

Characteristics of the duct array are

- an anisotropic behavior,
- no cross flow inside the duct,
- visco-thermal dissipation on the boundary layer,
- a certain flow inside the duct array.

## Modelling Methods

This chapter describes different modeling approaches. All Finite Element (FE) models are implemented in the commercial code Actran [5]. Three different modeling methods are discussed,

- Finite Element (FE) model of all components (FE model all components),
- Model the DPF with a Transfer Admittance (FE+TADM) as presented in [1]
- a homogenization for double fluid approach for the DPF (FE model double fluid).

The advantages and disadvantages for the different modeling approaches are listed below.

Modeling all components with a FE model requires meshing all components in detail. Provided the size of the ducts, the meshing task is complex and the resulting model requires significant computational time. The model achieves a high accuracy and is not limited by the frequency; see Figure 2, left side. This approach allows taking into account the mean flow.

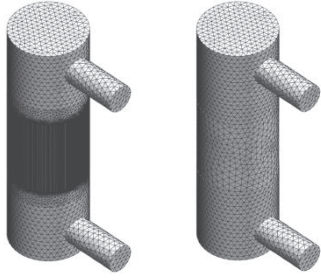


**Figure 2:** Shows the model approach FE model all components (left) and FE model double fluid (right), the homogenization approach allows reducing the model complexity with the same accuracy, see Results.

The second approach replaces the detailed FE model of the DPF substrate by transfer admittance (FE+TADM). The computational time is drastically reduced, but the model is globally less accurate than the complete model. In this model the mean flow cannot be taken into account. Additionally the transfer admittance needs to be computed for each frequency according to the most relevant analytical formulation for a given case.

The third approach describes the novel method to model the DPF in a homogenized way. This allows reducing modeling time, through simple mesh creation, see Figure 2. The accuracy is of the same level as for the detailed FE model of all components. This approach allows taking into account the mean flow.

### Double Duct Homogenization Approach

This chapter describes the driving equations of the homogenized duct array model. This approach uses the eXtended LRF (XLRF) equations to describe the sound wave propagation inside the duct array, respecting the mean flow [3], [4]. The XLRF has the following features,

- it uses the linearized Navier-Stokes equations,
- splits the coordinate system into propagation direction (pd) and cross direction (cd)
- uses plane wave hypothesis (valid as duct diameter is small).

The governing equation is the convected wave equation (1). It describes the wave propagation inside the small ducts.

$$\begin{aligned} \nabla \cdot \left( \frac{\Omega \underline{\underline{A}} (\|\tilde{c}\|^2 - \|\bar{v}\|^2)}{\tilde{\rho} \tilde{c}^2} \nabla \psi - i\omega \frac{\Omega \bar{v}}{\tilde{\rho} \tilde{c}^2} \psi \right) & \quad (1) \\ - i\omega \frac{\Omega \bar{v}}{\tilde{\rho} \tilde{c}^2} \cdot \nabla \psi + \frac{\Omega \omega^2}{\tilde{\rho} \tilde{c}^2} \psi & \\ = i\omega q + \nabla \cdot (\bar{v} q) & \end{aligned}$$

Equation (1) includes the porosity  $\Omega$  and the vector  $\underline{\underline{A}}$ , giving the duct orientation, the density  $\tilde{\rho}$  and the speed of sound  $\tilde{c}$  of the cross section,  $\bar{v}$  is the mean velocity,  $\psi$  the velocity potential,  $q$  the local volumetric source amplitude.

The XLRF propagation equations are coupled through a transfer admittance matrix term.

It includes

- the flow Resistivity  $R$  of the porous material, and
- the Fluid Bulk Modulus  $K$ .

The coupled physical values are the fluid pressure  $p$  and the volumetric source amplitude  $q$ ; see (2) and (3).

$$\begin{bmatrix} q_1 \\ q_2 \end{bmatrix} = \begin{bmatrix} T_{11} & T_{12} \\ T_{21} & T_{22} \end{bmatrix} \begin{bmatrix} p_1 \\ p_2 \end{bmatrix} \quad (2)$$

$$\begin{bmatrix} T_{11} & T_{12} \\ T_{21} & T_{22} \end{bmatrix} = \begin{bmatrix} \frac{1}{i\omega R} - \frac{1}{2K} & -\frac{1}{i\omega R} - \frac{1}{2K} \\ -\frac{1}{i\omega R} - \frac{1}{2K} & \frac{1}{i\omega R} - \frac{1}{2K} \end{bmatrix} \quad (3)$$

The values for the equivalent flow resistivity  $R$  and the equivalent bulk modulus  $K$  can be derived from the equations (4), (5), (6) and (7), with  $L_{DPF}$  the length of the DPF,  $R_{visco}$  the flow resistivity due to the small ducts,  $R_{wall}$  the flow resistivity and  $\Omega_{wall}$  the porosity of the porous material in-between the ducts (e.g. cordierite),  $t$  the wall thickness,  $a$  the duct width,  $\Omega_i$  the porosity of duct  $i$ ,  $K_i$  the fluid bulk modulus of duct  $i$ .  $R_{tot}$  is the total flow resistivity of the DPF and  $K_{tot}$  the total bulk modulus of the DPF. The equations (4), (5) and (6) (7) are linked by  $R_{tot}$  or  $K_{tot}$ .

$$R_{tot} = RL_{DPF} + R_{visco} \quad (4)$$

$$R_{tot} = \frac{R_{wall}}{\Omega_{wall}} \frac{t(a+t)^2}{2L_{DPF}a} + R_{visco} \quad (5)$$

$$1/K_{tot} = \frac{1}{K} + \frac{\Omega_1}{K_1} + \frac{\Omega_2}{K_2} \quad (6)$$

$$1/K_{tot} = \frac{\Omega_{wall}(1 - \Omega_1 - \Omega_2)}{K_{air}} + \frac{\Omega_1}{K_1} + \frac{\Omega_2}{K_2} \quad (7)$$

### Results

The model is tested on an example case for DPF. The dimensions of the DPF are shown in Figure 3. Based on equations (4) to (7) the values for the equivalent flow resistivity  $R$  and the equivalent bulk modulus  $K$  are computed. Their values are given in (8) and (9).

$$R = 30.43 \text{ Ns/m}^2 \quad (8)$$

$$K = 1532.68 \text{ kPa} \quad (9)$$

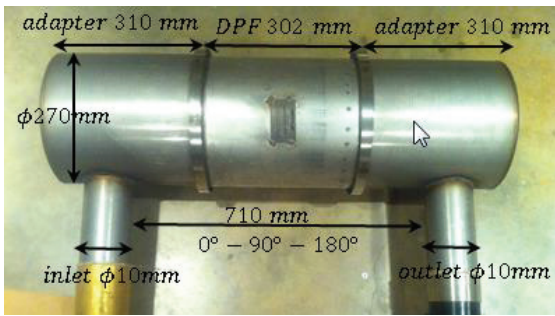


Figure 3 DPF measurement model

### Transmission Loss Results

The transmission loss (TL) is computed for 3 different model approaches and for the measurements, in brackets the label in the figures.

1. FE model of all components (TL p\_porous=0.3),
2. FE model double fluid (TL double fluid p\_porous=0.3),
3. FEM+TADM (FEM+TADM),
4. Measurements (experimental).

In all models the porosity of the cordierite is estimated to  $\Omega_{wall} = 0.3$ .

Figure 4 shows the Transmission Loss (TL) results. Model one (TL p\_porous=0.3) and model two (TL double fluid p\_porous=0.3) show correlation results of high quality.

The correlation is less good above 1800 Hz for all models. At this frequency other modes than the plane waves are cut-on in the inlet and outlet ducts. These modes are not injected in the numerical model because their amplitude was not characterized during the experiments. One has to note that higher order duct modes are supported by all three methods (FE model of all components, FE model Double Fluid, FEM+TADM).

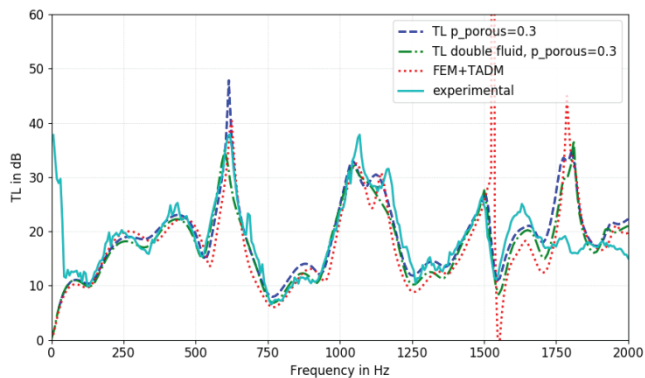


Figure 4 Transmission Loss Results of 3 different modeling methods compared to measurement results

Figure 4 show that the model FEM+TADM correlates slightly less with experiment, especially around 1500Hz. The offset of the FEM+TADM model to the measurements is increasing with frequency. This is shown more clearly in Figure 5.

Mean values and Root Mean Squared (RMS) values are computed from the difference of the simulation to the measurement, see Table 1. The FE model of all components

and the FE model Double Fluid have the same accuracy, FEM+TADM is less accurate.

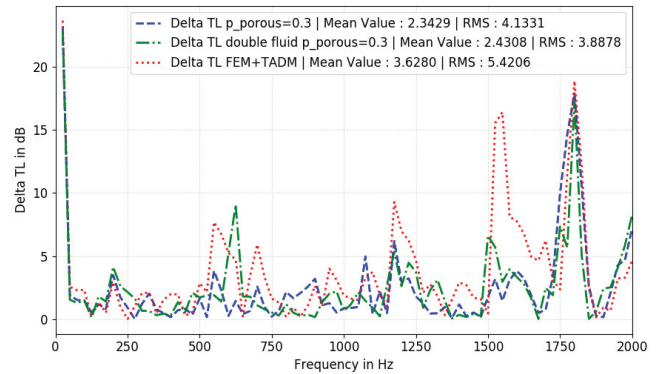


Figure 5: Delta TL values for each method compared to the measurement results

Table 1 Mean Error and RMS Error

	Mean Error	RMS Error
FE model of all components (Delta TL p_porous=0.3)	2.3 dB	4.1 dB
FE model double fluid (Delta TL double fluid p_porous=0.3)	2.4 dB	3.9 dB
FEM+TADM (Delta TL Fem+TADM)	3.6 dB	5.4 dB

### Influence of Mean Flow

The novel modelling approach (FE model Double Fluid) allows taking into account the mean flow in and outside of the DPF. As stated in [6] and [7] the mean flow has little influence on the results, except for low frequencies.

A flow profile is applied on the DPF. Figure 6 shows this flow profile. The maximum of the flow is  $\bar{v} = 10$  m/s at the duct array entry and exit, decreasing linearly to  $\bar{v} = 0$  m/s at the duct array other end.

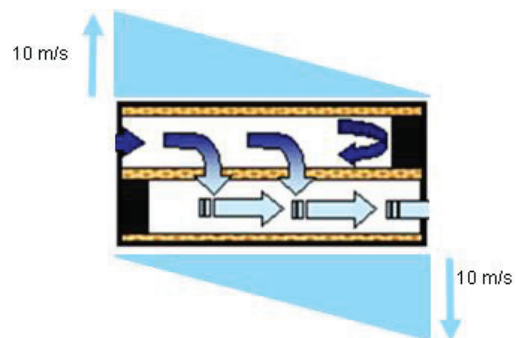
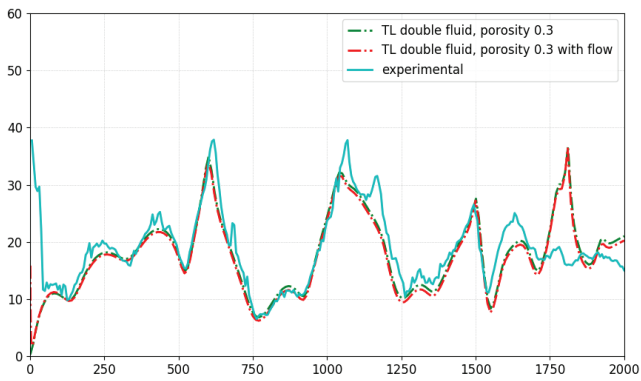
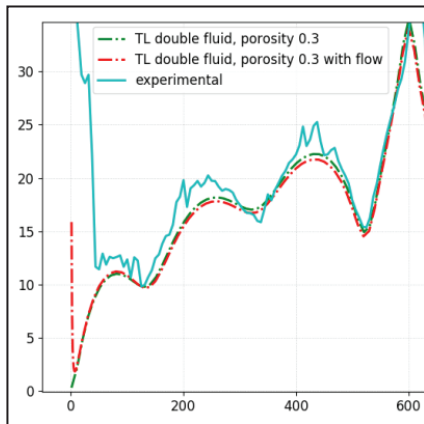


Figure 6: Flow profile applied on DPF tubes

The applied flow profile Figure 6 has low influence on the results as shown in Figure 7. Mean flow has only an impact at small frequencies. One notices that the trend of the measurements at low frequencies can be reproduced by including the mean flow in the simulation, see Figure 8.



**Figure 7:** Low influence of the flow profile over the entire frequency band, except for low frequencies



**Figure 8:** Influence of flow at low frequencies, the FE model Double Fluid with shows the same trend as the measurements

## Computational Requirements

The novel approach for the DPF with the FE model Double Fluid has the same accuracy as the detailed FE model of all components. But it reduces drastically the computational resources. The FE model Double Fluid uses 300 MB of memory and computational time is 1 second / frequency, compared to the detailed FE model of all components using 128 GB of RAM and 10 minutes to compute one frequency solution.

## Conclusions

A novel modeling method has been presented, allowing to model DPF with a highly accurate homogenized approach. This method could also be applied to air heat exchangers. In comparison to a very detailed FE model, the computational resources are much smaller by keeping the same accuracy.

This model allows accounting for mean flow inside the duct arrays which has an effect at very low frequencies. The entire model is implemented in the commercial code Actran [5].

## Acknowledgements

This work has been funded by the Silenthalpic Project of the Walloon Region, Belgium. We want to thank X. Hua from Kentucky University for the collaboration.

## Literature

- [1] Hua, X., Herrin D. W., Wu, T. W., Elnady T. (2012). Simulation of Diesel Particulate Filters in Large Exhaust Systems. Proceedings of the Internoise conference.
- [2] Lielens, G.: Acoustic modeling of DPF filters, SAPEM 2017
- [3] Beltman, W. M. (1998). Viscothermal wave propagation including acousto-elastic interaction. Department of Mechanical Engineering, University of Twente.
- [4] Sambuc, C., Lielens, G., & Coyette, J. P. (2014). Numerical modelling of visco-thermal acoustics using finite elements. In *Proceedings of the ISMA*.
- [5] Free Field Technologies, Actran 18 User's guide: Vol2, 2017.
- [6] Mukherjee, N. K. (2009). Flow-Acoustic Analysis of Diesel Particulate Filter and Air Filter (Doctoral dissertation, Indian Institute of Science Bangalore).
- [7] Falk Lissel, L., & Kristoffersson, J. (2011). Acoustical properties for diesel particulate filters.